*Carnegie Observatories Astrophysics Series, Vol. 3:
Clusters of Galaxies: Probes of Cosmological Structure and Galaxy Evolution, 2004
ed. J. S. Mulchaey, A. Dressler, and A. Oemler (Pasadena; Carnegie Observatories:
http://www.ociw.edu/ociw/symposia/series/symposium3/proceedings.html)*

A New Galaxy Cluster Survey For The Northern Sky

R. R. GAL[1] et al.
(1) Johns Hopkins University, Baltimore, MD USA

Abstract
We present a new galaxy cluster catalog constructed from the Digitized Second Palomar Observatory Sky Survey. Our objectively defined catalog covers the entire Northern sky at $|b| > 30°$, and contains nearly 20,000 cluster candidates with photometric redshifts and richnesses. Extensive simulations are used to establish contamination rates and our selection function. We also present some initial work on cluster mass estimation directly from our plate photometry.

1.1 The Northern Sky Optical Cluster Survey

The Northern Sky Optical Cluster Survey (Gal et al. 2003) is a new, objectively defined catalog of candidate galaxy clusters based on the galaxy catalogs from the Digitized Second Palomar Observatory Sky Survey (DPOSS, Djorgovski et al. 1999). The final cluster catalog covers almost 12,000 square degrees with nearly 16,000 candidate clusters at $z < 0.3$. The catalog is built from three distinct regions: the Northern Galactic Cap well-calibrated plates (NGP-good), Southern Galactic Cap (SGP) plates, and NGP poorly calibrated plates (NGP-poor). As demonstrated below, the catalogs from these three areas are statistically identical.

In all cases, we use catalogs of galaxies with $r < 19.5$, and require a g detection to remove spurious objects. A simple adaptive kernel density mapping technique is used to generate images of the projected galaxy density, upon which object detection is performed with SExtractor. These "objects" are in fact galaxy overdensities, which we identify as clusters.

In Figure 1, we show the complete cluster catalog with plate boundaries outlined.

Following Postman et al. (2002), we use the Rayleigh-Levy (RL) distribution to generate simulated galaxy catalogs, upon which the same algorithm is run to estimate the false positive (contamination) rate. For each plate in the survey, we set the SExtractor detection thresholds such that the contamination rate C is 10%, while maximizing the total number of detections. This forces a constant C across the sky, but results in variable detection efficiency between plates. To assess the selection function for each plate, we use simulated galaxy clusters spanning a range of richness and redshift, which are placed in the actual background field derived from the respective plate. These galaxy catalogs consisting of a background plus artificial clusters are used to generate density maps on which we run SExtractor, with the same detection parameters used for the real cluster detections. This procedure allows us to measure the selection function for each plate, an example of which is shown in the left panel of Figure 6.

Photometric redshifts are derived using an empirical relation between spectroscopic red-

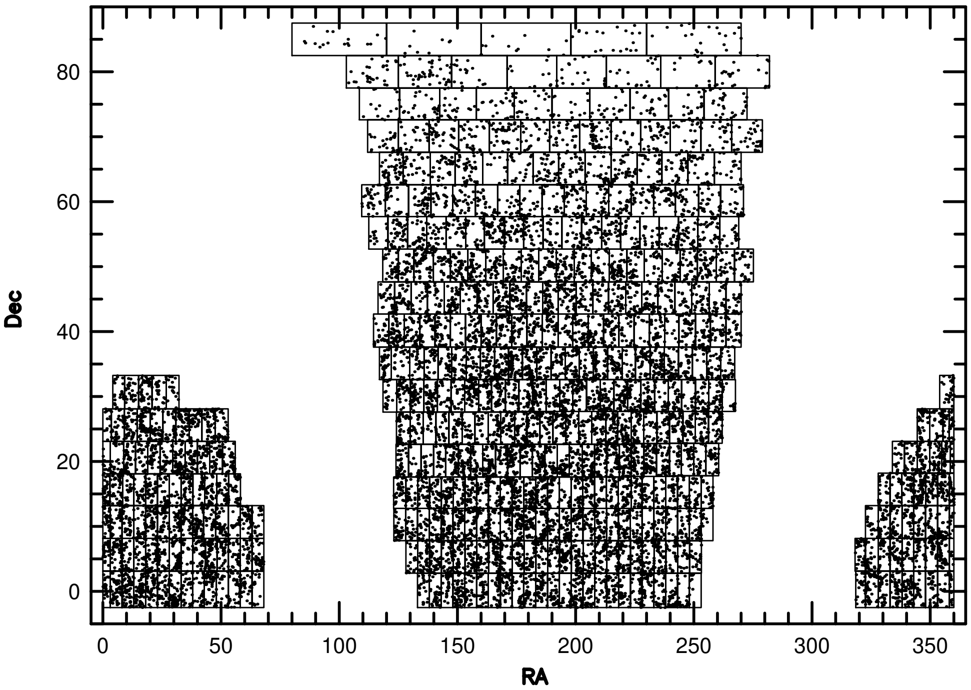

Fig. 1.1. The NoSOCS Cluster Catalog with plate boundaries.

shift taken from the literature (Struble & Rood 1999), and the median $g-r$ color and mean r magnitude of the background-corrected galaxy population inside a radius of 1 Mpc ($0.67 \times R_{Abell}$) for each candidate. This procedure yields redshift estimates accurate to $\Delta z = 0.033$. Given a redshift estimate for each cluster, we can measure a richness that samples the same absolute magnitude range. We compute the richness in a fixed absolute magnitude interval, $M_r^* - 1 < M < M_r^* + 2$, using the r-band data, and assuming $M_r^* = -21.53$, taken from the cluster luminosity functions derived by Paolillo et al. (2001). Galaxies are counted within a radius of $1h^{-1}$ Mpc. For distant clusters where the faint end of the magnitude range extends beyond our catalog limits, a correction is applied. The median redshift of our sample is $z_{med} = 0.1579$, which corresponds well to the value anticipated based on the magnitude coverage of our galaxy catalog. The median richness for our clusters is $N_{gals,med} = 31$, which corresponds to the poorest end of Abell's richness class 0. We therefore expect that our catalog contains many very poor clusters (or even groups). Figure 2 shows redshift and richness distributions, for our entire sample as well as subsamples in richness and redshift, respectively. As expected, poor clusters are seen only at the lowest redshifts.

Because the three regions of our survey are cataloged independently (but using the identical methodology), we must ensure that the resulting cluster catalogs do not contain any systematic errors. In Figure 3, we compare the (scaled) redshift and richness distributions for the three subsamples; clearly, they are extremely similar.

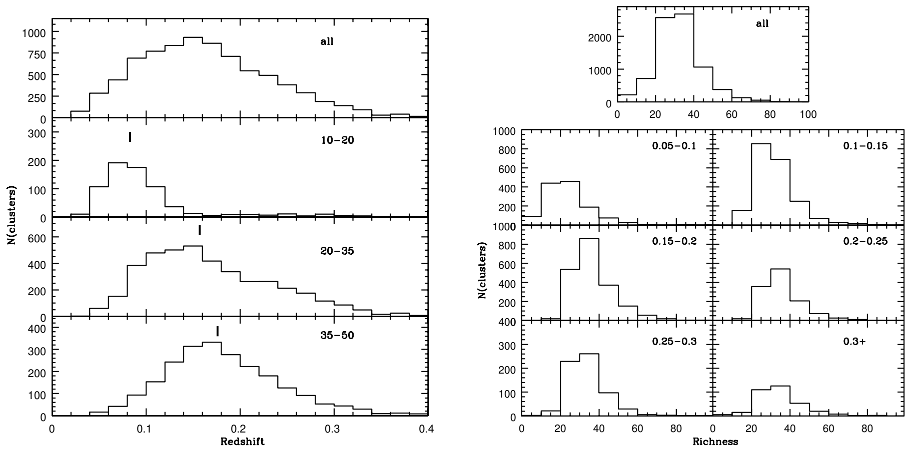

Fig. 1.2. Redshift distributions (left) and richness distributions (right) for our cluster sample.

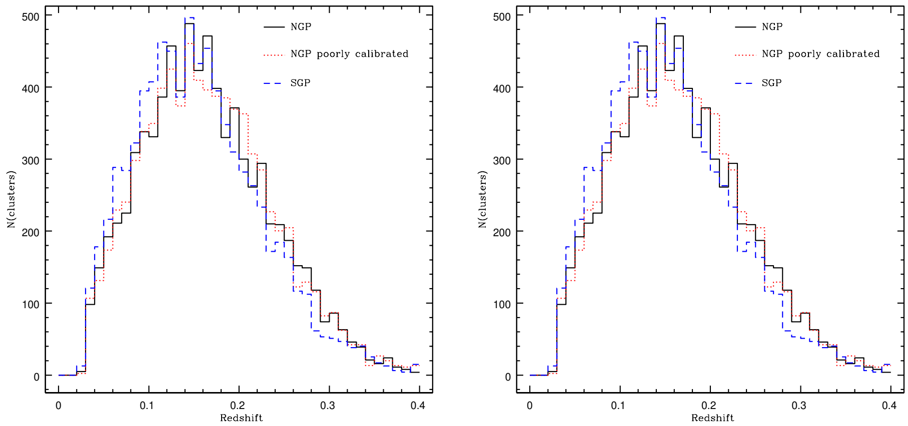

Fig. 1.3. Redshift distributions (left) and richness distributions (right) for the three regions defining our cluster sample.

1.2 Mass Estimation

A fundamental physical property of galaxy clusters is their mass. Mass can be measured using X-ray data, velocity dispersions, lensing (strong and weak); all of these methods require data which is difficult to obtain for extremely large cluster samples, and often impossible for low-mass systems. One expects that the number of galaxies in a cluster (the cluster richness) should be correlated with the total cluster mass. Unfortunately, cluster richnesses are notoriously difficult to measure, and there are a variety of different estimators. First, we would like to know if our richness measure, N_{gals}, is correlated with any other *optical* richness estimator. Comparison to Λ_{cl} from Kim (2001) shows excellent agreement, especially considering that the measures are independent, the base catalogs are different (DPOSS and SDSS), the redshifts are photometric in both cases and may not agree, the cluster centers may differ, and the photometry is independent. This comparison is shown in Figure 4. Open circles are clusters where the photometric redshifts disagree.

The above comparison provides some confidence that these two optical richness measures

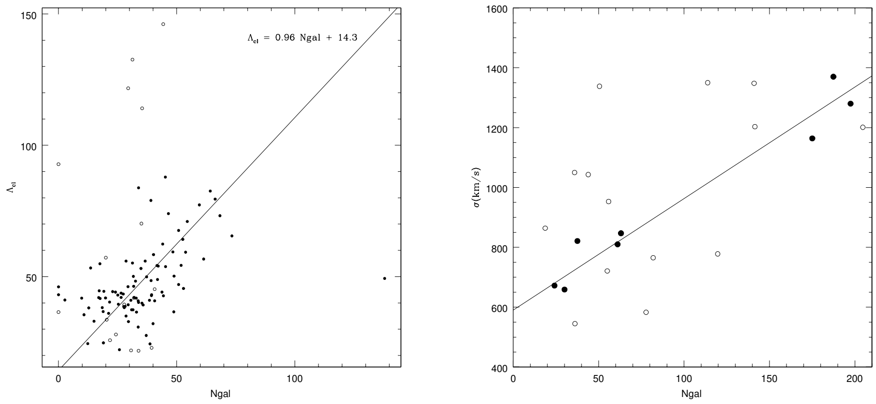

Fig. 1.4. *Left:* Our richness measure N_{gals} compared to Λ_{cl} from Kim (2001). *Right:* The $N_{gal} - \sigma$ relation for clusters with $n_z > 60$. Filled circles are clusters with regular profiles, open circles have irregular profiles.

at least measure similar global cluster properties. But is that property related to mass? In Figure 5, we compare our richness measure (as well as an alternative, Dn) with velocity dispersions taken from the literature. On the left, we show clusters with 25 or more redshifts, and on the right, we require sixty redshifts for a velocity dispersion. A further, and perhaps more important factor is the cluster radial profile; irregular clusters deviate strongly from a clean relation, as shown in the right panel of Figure 4. Such stringent requirements limit the number of useful clusters, and show the need for great caution in these studies.

Applying our richness-mass relation to the NGP-good area, and a preliminary completeness correction (based on our selection functions, an example of which is shown in the left panel of Figure 6), we estimate the density of clusters with $\sigma > 800 kms^{-1}$ at $z \sim 0.15$. We use the technique of Postman et al. 2002. Error bars reflect only Poissonian errors. Increasing the area surveyed will significantly improve our measurement. As shown in the right panel Figure 6, we agree well with the low-redshift result from CNOC (from 3 clusters). A major point is the inclusion of all clusters regardless of radial profile, even though the conversion to mass comes from regular clusters only. Thus, σ_8 may be overestimated because non-relaxed clusters have their mass overestimated. We conclude that extreme caution must be used when deriving mass estimates directly from photometric cluster properties; even with spectroscopy, a large number of redshifts are necessary to understand cluster kinematics.

References

Borgani, S., Girardi, M., Carlberg, R. G., Yee, H. K. C., & Ellingson, E. 1999, ApJ, 527, 561

Djorgovski, S. G., Odewahn, S. C., Gal, R. R., Brunner, R., de Carvalho, R. R., Longo, G. & Scaramella, R. 1999, American Astronomical Society Meeting, 194, 0414

Gal, R. R., de Carvalho, R. R., Odewahn, S. C., Djorgovski, S. G., Mahabal, A., Brunner, R. J. & Lopes, P. 2003, AJ, *in press*

Kim, R. S. J. 2001, Ph.D. Thesis, Princeton

Paolillo, M., Andreon, S., Longo, G., Puddu, E., Gal, R. R., Scaramella, R., Djorgovski, S. G., & de Carvalho, R. 2001, A&A, 367, 59

Postman, M., Lauer, T. R., Oegerle, W., & Donahue, M. 2002, ApJ, 579, 93

Struble, M. F. & Rood, H. J. 1999, ApJS, 125, 35

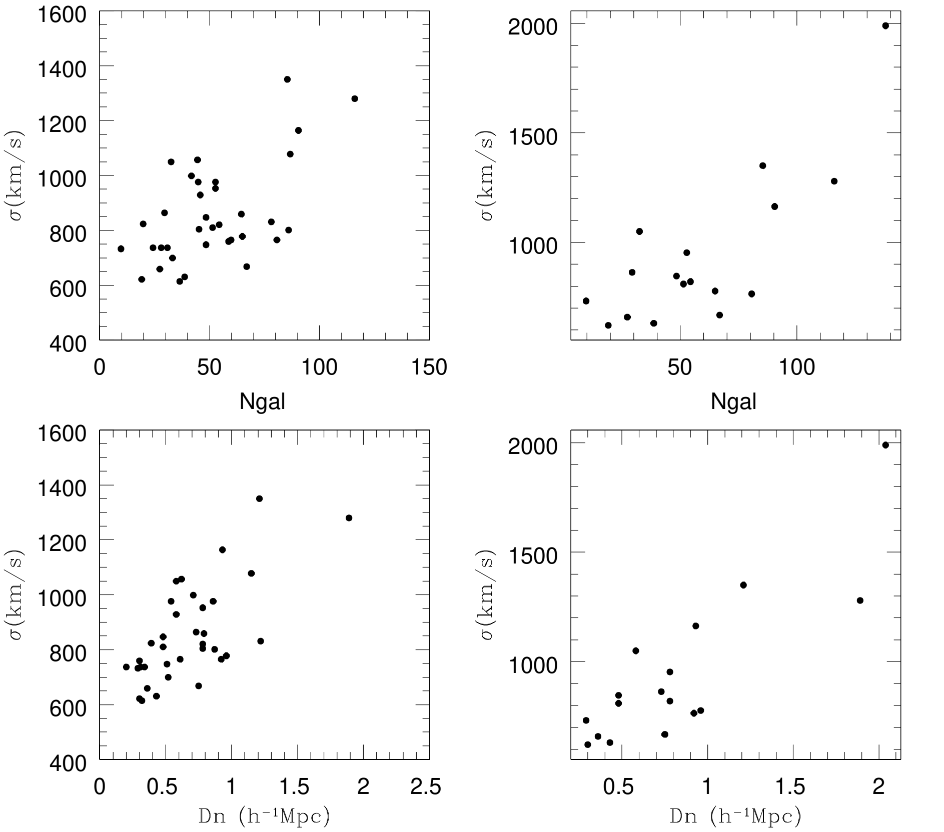

Fig. 1.5. Richness estimates vs. velocity dispersion, for clusters with > 25 redshifts (left) and > 60 redshifts as well as regular radial profiles (right).

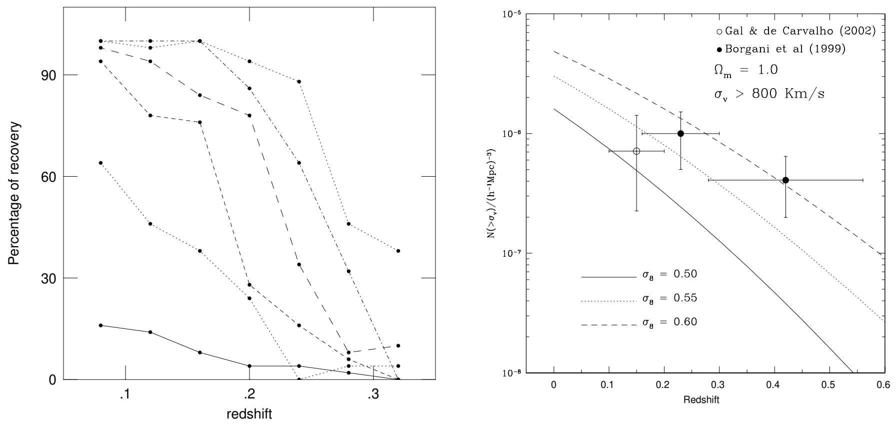

Fig. 1.6. *Left:* An example selection function for one DPOSS plate. *Right:* A preliminary cluster mass function, using our data at $z = 0.15$ and the CNOC results at higher redshift. Note that the value of Ω_m used results in low σ_8.